Illustrating the effect of physicochemical properties within vitrinite and inertinite on residual carbon formation in drop tube furnace

Hua Ma[1], Yonghui Bai [1, *], Xiaoyong Men [2], Qingyun Wang [1], Xudong Song [1], Peng Lv [1], Jiaofei Wang [1], Guanghua Lu [3], Guangsuo Yu [1, 4]

1 State Key Laboratory of High–Efficiency Utilization of Coal and Green Chemical Engineering, College of Chemistry and Chemical Engineering, Ningxia University, Yinchuan 750021, China

2 CHN Energy Ningxia Coal Industry Co., Ltd., Yinchuan 750000, China

3 Chemical Engineering, University of Newcastle, Callaghan, NSW 2308, Australia

4 Institute of Clean Coal Technology, East China University of Science and Technology, Shanghai 200237, China

**Corresponding author. Tel: 0951–2062008.*

E–mail: yhbai@nxu.edu.cn

Highlights

- Residual carbon formation from entrained-flow gasification fine slag was revealed.
- Vitrinite is prone to achieve a higher conversion level at entrained-flow conditions.
- Vitrinite residual carbon has more active sites, giving a higher gasification activity.

1. Introduction

Entrained flow coal gasification technology is widely used in the field of coal gasification technology [1-2] while it will produce a large amount of fine slag, which causes environmental pollution, energy waste and other problems [3]. Therefore, the residual carbon of gasification reaction with different macerals was prepared under rapid heating conditions in this study, and the carbon conversion and physicochemical structures were analyzed, which could help to deepen the understanding of the correlation between microstructure of the coal and macroscopic reaction properties.

2. Methods

In this study, Meihuajing coal was selected to be separated and enriched macerals by density gradient centrifugation and different macerals were gasified at 1300 °C and H_2O/O_2 conditions in the drop tube furnace (DTF, **Figure 1**) to collect residual carbon.

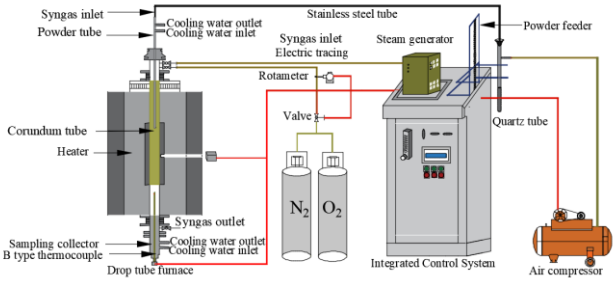

Figure 1. Schematic diagram of the heating device of the DTF

3. Results and discussion

The carbon conversion was calculated by using Eqn. (1) for the collected residual carbon, where M_0 was actual inlet quality of maceral enrichments in the dry and ash–free basis, and M was the quality of residual carbon collected after the gasification, carbon conversion of the bar graph was shown in **Figure 2.** It could be found that the carbon conversion of MHJ – V and MHJ – I were 69.94 % and 58.26 %, while Δ_2 gave a difference of 4.71 % between the volatile content of the two, and it was obvious

that Δ_1 was much larger than Δ_2, which implied that the carbon structure of the coal maceral enrichments contributes more to their conversion. Overall, MHJ – V reacted more deeply compared to MHJ – I under the entrained–flow conditions.

$$\text{Xdaf} = \frac{M_0 - M}{M_0} \tag{5}$$

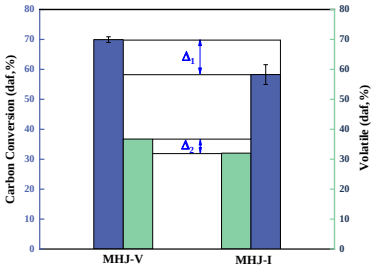

Figure 2. Volatile content and carbon conversion of different maceral enrichments

Scanning electron microscope was used to observe the surface morphology of different maceral enrichments and residual carbon, as shown in **Figure 3**. It could be seen that the surface of MHJ – V was relatively smooth and flat with densely arranged particles, while the surface of MHJ – I was rougher, which might be due to the fact that some of the minerals were not completely removed were assigned to the MHJ – I in various forms. Observing the surface morphology of residual carbon, the surface of MHJ – VC was severely corroded, a large number of porous structures appeared, presenting a clear honeycomb structure, while some clearly visible small microporous appeared on the surface of MHJ – IC. The above results were consistent with the carbon conversion of maceral enrichments in **Figure 2**, indicating that MHJ – V was more likely to realize the gasification reaction under high temperature, short residence time and H_2O/O_2 gasification conditions.

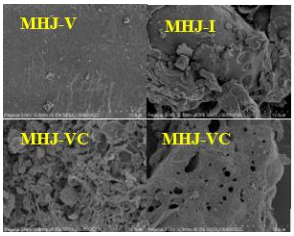

Figure. 3 Micromorphology of maceral enrichments and residual carbon

XRD was used to characterize the microcrystalline structure of the residual carbon of different maceral enrichments under rapid heating conditions, and the stacked aromatic lamellae similar to the graphite (semi – graphite) structure was called "microcrystals", as shown in **Figure 4**, which showed that the peaks of 002 and 100 of residual carbon are prominent compared with those of the original maceral enrichments, implying that the high – temperature gasification process had led to the development of the carbon structure in the direction of ordering [4].

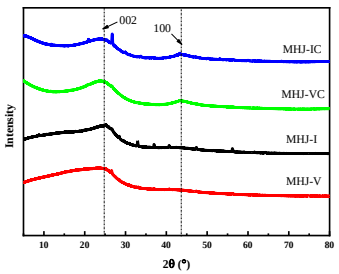

Figure. 4 XRD patterns of maceral enrichments and residual carbon

To further understand the differences in chemical structure of the residual carbon of different maceral enrichments, the carbon microcrystalline structure parameters were given in **Table 5**. The

aromatic lamellae diameters (La) and stacking heights (Lc) of MHJ – I were higher than those of MHJ – V, suggesting that the aromatic rings of MHJ – I had a higher degree of condensation and graphitization. Due to the shedding of aliphatic side chains and oxygen – containing functional groups, the Lc of MHJ – IC increased, and the number of aromatic lamellae stacked increased, which led to the decrease of the d002 and the closer arrangement of the macromolecular structure, at the same time Lc and La of MHJ – IC were higher than those of MHJ – VC, indicating that the ordering process of carbon microcrystalline structure of MHJ – IC was faster at higher gasification temperature and H_2O/O_2 conditions.

Table. 5 Structural parameters of carbon microcrystals

Sample	$fa = \frac{A002}{A002 + A\gamma}$	$Lc = \frac{K_c\lambda}{B_{002}\cos\theta_{002}}$	$La = \frac{K_a\lambda}{B_{100}\cos\theta_{100}}$	$d_{002} = \frac{\lambda}{2\sin\theta_{002}}$
MHJ – V	0.267	1.125	2.038	0.362
MHJ – I	0.396	1.160	2.714	0.361
MHJ – VC	0.724	1.156	2.943	0.358
MHJ – IC	0.834	1.256	3.161	0.350

Note[5,6]: λ – the wavelength of Cu Kα rays (nm) was used, λ = 0.154056 nm;

θ_{002}, θ_{100} – the diffraction angle (°) corresponding to the 002 and 100 peaks;

β_{002}, β_{100} – half peak width values (rad) for peaks 002 and 100;

K_c, K_a – constants, K_c = 0.89, K_a = 1.84

4. Conclusions

Under rapid heating conditions, compared with the Inertinite residual carbon, the vitrinite residual carbon has a richer pore structure, a larger specific surface area, a lower degree of graphitization, and a higher reactivity.

References

[1] X. Wu, Q. Guo, Y. Gong, et al, 2022. Influence of burner geometry on atomization of coal water slurry in an entrained–flow gasifier. Chem. Eng. Sci. 247, 117088

[2] F. Weiland, P.T. Nilsson, H. Wiinikka, et al, 2014. Online characterization of syngas particulates using aerosol mass spectrometry in entrained–flow biomass gasification. Aerosol Science and Technology. 48(11), 1145–1155

[3] G. Dai, S. Zheng, X. Wang, et al, 2020. Combustibility analysis of high–carbon fine slags from an entrained flow gasifier. Journal Of Environmental Management. 271, 111009

[4] X. Zhang, X. Song, W. Su, et al, 2019. In–situ study on gasification reaction characteristics of Ning Dong coal chars with CO_2. Journal of Fuel Chemistry and Technology. 47(4), 385–392

[5] X. Li, M. An, Q. Guo, 2020. Reactivity and structure evaluation of coal chemical looping gasification based on Cu–Fe oxygen carrier. Acta Petrol Sin. 36, 1306–1311.

[6] N. Mohammad, F. Mohammad, S. John, 2002. Use of X–ray diffraction in assessing the aging pattern of asphalt fractions. Fuel. 81, 51–58

Keywords

Entrained–flow gasification; Fine slag; Macerals; Residual carbon